Available online at www.sciencedirect.com
ScienceDirect
Dyes and Pigments 77 (2008) 315–322
DYES and PIGMENTS
www.elsevier.com/locate/dyepig

The effect of the inclusion of guest molecules on the solid-state fluorescence of naphthooxazole-type fluorophores

Yousuke Ooyama*, Kunimitsu Nonami, Shigeru Watanabe, Katsuhira Yoshida**

Department of Material Science, Faculty of Science, Kochi University, Akebono-cho, Kochi 780-8520, Japan

Received 3 March 2007; received in revised form 10 May 2007; accepted 15 May 2007
Available online 12 June 2007

Abstract

Although naphthooxazole-type fluorophores did not exhibit fluorescence in solution, they exhibited strong fluorescence in the solid state. Interestingly, a large red-shift in colour and drastic decrease in fluorescence intensity were observed upon inclusion of guest molecules in the crystalline state. To elucidate the enclathrated guest effects on the solid-state photophysical properties, the X-ray crystal structures of the guest-free and several guest-inclusion crystals have been determined. Semi-empirical molecular orbital calculations (PM3 and INDO/S) confirmed that the reasons for the red-shift of the absorption and fluorescence wavelength maxima and drastic fluorescence quenching behaviour upon formation of host–guest inclusion compounds are attributable to strong intermolecular π–π interactions and to the formation of continuous molecular linking by intermolecular hydrogen bonds.

Keywords: Fluorescence; Dyes; Inclusion compounds; Crystal structures; Heterocycles

1. Introduction

The solid-state fluorescence of organic fluorescent dyes has recently received considerable attention because of their potential use in the construction of optoelectronic devices [1–10]. To design solid-state emissive materials, it is important to obtain information about the relationship between the photophysical properties and the chemical and crystal structures of fluorophores. An organic fluorescent host which can exhibit sensitive colour and fluorescence changes upon formation of host–guest inclusion complexes is a good candidate for elucidation of the solid-state photophysical properties. Recently, Stalke and coworkers reported that disubstituted anthracene 9,10-$(Ph_2P{=}S)_2C_{14}H_8$ exhibits a dramatic fluorescence enhancement upon inclusion of toluene molecules in the crystalline state [11]. In contrast the present workers have developed novel benzofurano[3,2-*b*]naphthoquinol-type [12–14], imidazo[5,4-*a*]-anthraquinol-type [15,16] and phenanthro[9,10-*d*]-imidazole-type [17] fluorescent host crystals which exhibit dramatic fluorescence enhancement upon inclusion of various gaseous amines, organic solvents and carboxylic acids, respectively.

In this paper, the enclathrated guest effects on the solid-state photophysical properties and crystal packing of naphthooxazole-type fluorophores **2** are discussed on the basis of the results of semi-empirical molecular orbital calculations (PM3 and INDO/S) and X-ray crystal structure.

2. Experimental

IR spectra were recorded on a JASCO FT/IR-5300 spectrophotometer for samples in KBr pellet form. Absorption spectra were observed with a JASCO U-best30 spectrophotometer. For the measurement of the solid-state fluorescence excitation and emission spectra of the crystals, a JASCO FP-777 spectrometer equipped with a JASCO FP-1060 attachment was used. Single-crystal X-ray diffraction was performed on Rigaku

* Corresponding author. Fax: +81 88 844 8359.
** Corresponding author.
E-mail addresses: yooyama@hiroshima-u.ac.jp (Y. Ooyama), kyoshida@cc.kochi-u.ac.jp (K. Yoshida).

0143-7208/$ - see front matter © 2007 Elsevier Ltd. All rights reserved.
doi:10.1016/j.dyepig.2007.05.018

AFC7S diffractometer. Elemental analyses were recorded on a Perkin Elmer 2400 II CHN analyzer. ^{1}H NMR spectra were recorded on a JNM-LA-400 (400 MHz) FT NMR spectrometer with tetramethylsilane (TMS) as an internal standard. Column chromatography was performed on silica gel (KANTO CHEMICAL, 60N, spherical, neutral) or alumina (WAKO, about 300 mesh). Semi-empirical molecular orbital (MO) calculations were performed on FUJITSU FMV-ME4/657 by using the WinMOPAC ver. 3 package (Fujitsu, Chiba, Japan).

2.1. Synthesis of 4-[(4-diethylamino)phenylamino]-[1,2]naphthoquinone (**1a**)

To a solution of 1,2-naphthoquinone-4-sulfonic acid sodium salt (9.48 g, 36.4 mmol), sodium acetate (9.91 g, 72.8 mmol), and $NiCl_2$ (4.72 g, 36.4 mmol) in acetic acid (25 ml) was added, dropwise, a solution of *N*,*N*-diethyl-1, 4-phenylenediamine dihydrochloride (8.64 g, 36.4 mmol) in acetic acid (25 ml) with stirring at room temperature. After further stirring for 3 h, the reaction mixture was poured into water. The solution was neutralized with aq. Na_2CO_3 and the resulting precipitate was filtered, washed with water and dried to yield 9.10 g (78%) of **1a** as a blue solid: 229–231 °C (decomposition); ^{1}H NMR (400 MHz, DMSO-d_6, TMS): $\delta = 1.11$ (t, 6H), 3.42 (q, 4H), 5.63 (s, 1H), 6.75 (d, $J = 8.05$ Hz, 2H), 7.14 (d, $J = 8.05$ Hz, 2H), 7.70–7.72 (m, 1H), 7.83–7.85 (m, 1H), 8.02 (d, 1H), 8.29 (d, 1H), 9.77 (s, 1H); IR (KBr): $\tilde{\nu} = 3219,\ 1593,\ 1568\ cm^{-1}$; elemental analysis calcd (%) for $C_{20}H_{20}N_2O_2$: C 74.98, H 6.29, N, 8.74; found: C 74.77, H 6.11, N 8.87.

2.2. Synthesis of 4-[(4-diethylamino)-2-(methyl)phenylamino]-[1,2]naphthoquinone (**1b**)

To a solution of 1,2-naphthoquinone-4-sulfonic acid sodium salt (2.0 g, 7.68 mmol), sodium acetate (2.09 g, 7.68 mmol), and $NiCl_2$ (1.00 g, 7.68 mmol) in acetic acid (25 ml) was added dropwise a solution of *N*,*N*-diethyl-2-methyl-*p*-phenylenediamine monohydrochloride (1.65 g, 7.68 mmol) in acetic acid (25 ml) with stirring at room temperature. After further stirring for 7 h, the reaction mixture was poured into water. The solution was neutralized with aq. Na_2CO_3 and the resulting precipitate was filtered, washed with water and dried to yield 1.44 g (56%) of **1b** as a blue solid: ^{1}H NMR (400 MHz, DMSO-d_6, TMS): $\delta = 1.11$ (t, 6H,), 2.13 (s, 3H), 3.42 (q, 4H), 5.74 (s, 1H), 6.59–6.64 (m, 2H), 6.96 (d, 1H), 7.69–7.73 (m, 1H), 7.83–7.86 (m, 1H), 8.02 (d, 1H), 8.32 (d, 1H), 9.66 (s, 1H); IR (KBr): $\tilde{\nu} = 3210,\ 1598,\ 1575\ cm^{-1}$; elemental analysis calcd (%) for $C_{21}H_{22}N_2O_2$: C 75.42, H 6.63, N, 8.38; found: C 75.33, H 6.51, N 8.57.

2.3. 4-[5-(4-diethylamino-phenylamino)-naphtho-[1,2-d]oxazol-2-yl]benzonitrile (**2a**)

To a solution of the compound **1a** (5.00 g, 15.6 mmol) and ammonium acetate (24.05 g, 0.31 mol) in acetic acid (170 ml) was added dropwise a solution of *p*-cyanobenzaldehyde (2.05 g, 15.6 mmol) in acetic acid (100 ml) with stirring at 90 °C. After further stirring for 3 h, the reaction mixture was neutralized with aq. Na_2CO_3 and the product was extracted with CH_2Cl_2. The organic extract was washed with water and evaporated. Then the residue was chromatographed on silica gel (CH_2Cl_2:ethyl acetate = 10:1 as eluent) to give **2a** (4.86 g, yield 72%) as a yellow powder: m.p. 205–206 °C; ^{1}H NMR (400 MHz, DMSO-d_6, TMS): $\delta = 1.11$ (t, 6H), 3.35 (q, 4H), 6.76 (d, $J = 9.03$ Hz, 2H), 6.99 (s, 1H), 7.16 (d, 2H), 7.76 (t, 1H), 7.74 (t, 1H), 8.02 (d, 2H), 8.26–8.28 (m, 2H), 8.31 (s, 1H), 8.39 (d, $J = 8.29$ Hz, 1H), 8.48 (d, $J = 8.29$ Hz, 1H); IR (KBr): $\tilde{\nu} = 3404,\ 2224\ cm^{-1}$; elemental analysis calcd (%) for $C_{28}H_{24}N_4O$: C 77.75, H 5.59, N, 12.95; found: C 77.74, H 5.59, N 12.98.

2.4. 4-[5-(4-diethylamino-2-methyl-phenylamino)-naphtho[1,2-d]oxazol-2-yl] benzonitrile (**2b**)

To a solution of the compound **1b** (1.00 g, 2.99 mmol) and ammonium acetate (3.69 g, 47.8 mmol) in acetic acid (25 ml) was added dropwise a solution of *p*-cyanobenzaldehyde (0.39 g, 2.99 mmol) in acetic acid (25 ml) with stirring at 90 °C. After further stirring for 3 h, the reaction mixture was neutralized with aq. Na_2CO_3 and the product was extracted with CH_2Cl_2. The organic extract was washed with water and evaporated. Then the residue was chromatographed on silica gel (CH_2Cl_2:ethyl acetate = 3:1 as eluent) to give **2b** (4.86 g, yield 52%) as a yellow powder: ^{1}H NMR (400 MHz, DMSO-d_6, TMS): $\delta = 1.12$ (t, 6H), 2.11 (s, 3H), 3.35 (q, 4H), 6.32 (s, 1H), 6.61 (dd, 1H), 6.68 (d, 1H), 7.03 (d, 1H), 7.59 (t, 1H), 7.73 (t, 1H), 7.98 (d, 2H), 8.10 (s, 1H), 8.22 (d, 2H), 8.37 (d, 1H,), 8.52 (d, 1H); IR (KBr): $\tilde{\nu} = 3387,\ 2230\ cm^{-1}$; elemental analysis calcd (%) for $C_{29}H_{26}N_4O$: C 78.00, H 5.87, N, 12.55; found: C 77.70, H 5.86, N 12.31.

2.5. Computational methods

All calculations were performed on FUJITSU FMV-ME4/657; semi-empirical calculations were carried out using the WinMOPAC ver. 3 package (Fujitsu, Chiba, Japan). Ground state geometrical calculations were carried out using the PM3 method [18]; all geometries were completely optimized. The absorption spectra of the seven quinol derivatives were studied using the semi-empirical, intermediate neglect of differential overlap/spectroscopic(INDO/S) [19–21] employing single excitation full SCF/CI (self-consistent field/configuration interaction), which includes the configuration of one electron excited from any occupied orbital to any unoccupied orbital; 225 configurations were considered for the configuration interactions.

2.6. Preparation of guest-inclusion crystals

The host compound **2a** or **2b** was dissolved with heating in the respective guest solvent. The ensuing solution was filtered,

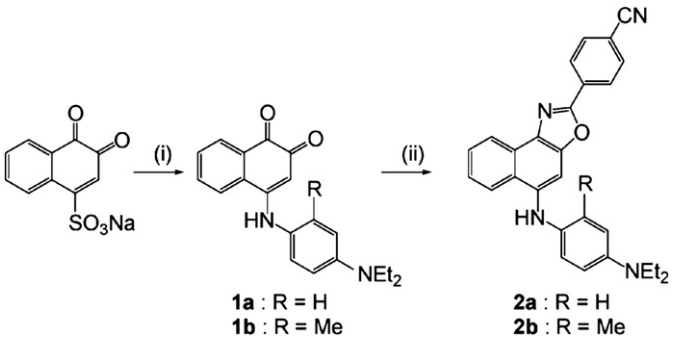

Scheme 1. (i) **1a**: *N*,*N*-diethyl-1,4-phenylenediamine dihydrochloride, CH_3COONa, $NiCl_2$, CH_3COOH, 3 h, RT, 78%; **1b**: *N*,*N*-diethyl-2-methyl-1,4-phenylenediamine, CH_3COONa, $NiCl_2$, CH_3COOH, 7 h, RT, 56%; (ii) *p*-cyanobenzaldehyde, CH_3COONH_4, CH_3COOH, 3 h, 90 °C, 72% for **2a**, 52% for **2b**.

kept for a few days at room temperature and the crystals that formed were collected by filtration. The host:guest stoichiometric ratio of the inclusion compounds was determined by means of ^1H NMR integration and CHN analysis.

2.7. X-ray crystallographic studies

The reflection data were collected at 23 ± 1 °C on a Rigaku AFC7S four-circle diffractometer by $2\theta-\omega$ scan technique, and using graphite-monochromated Mo Kα ($\lambda = 0.71069$ Å) radiation at 50 kV and 30 mA. In all cases, the data were corrected for Lorentz and polarization effects. A correction for secondary extinction was applied. The reflection intensities were monitored by three standard reflections for every 150 reflections. An empirical absorption correction based on azimuthal scans of several reflections was applied. All calculations were performed using the teXsan [22] crystallographic software package of Molecular Structure Corporation. CCDC-630058 (**2a**) and CCDC-630059 (**2a**·acetone) contain the supplementary crystallographic data for this paper. These data can be obtained free of charge from The Cambridge Crystallographic Data Centre via www.ccdc.cam.au.uk/data_request/cif.

2.7.1. Compound *2a*

Crystals of **2a** were recrystallized from ethanol as yellow needles, and were air stable. The one selected had approximate dimensions 0.60 × 0.20 × 0.40 mm. The transmission factors ranged from 0.96 to 0.99. The crystal structure was solved by direct methods using SIR 92 [23]. The structures were expanded using Fourier techniques [24]. The non-hydrogen atoms were refined anisotropically. Some hydrogen atoms were refined isotropically, the rest were fixed geometrically and not refined. *Crystal data*: $C_{28}H_{24}N_4O$, $M = 432.52$, triclinic, $a = 10.530(1)$, $b = 15.062(1)$, $c = 7.425(1)$ Å, $\alpha = 96.555(8)°$, $\beta = 105.994(9)°$, $\gamma = 86.429(8)°$, $U = 1124.0(2)$ Å^3, $T = 296.2$ K, space group $P1$ − (no.2), $Z = 2$, μ(Mo Kα) = 0.80 cm^{-1}, 4195 reflections measured, 4191 unique ($R_{int} = 0.018$) which were used in all calculations. The final R indices were $R_1 = 0.069$, $wR(F^2)$ was 0.190 (all data).

Crystals of **2a** were recrystallized from acetone as red prisms; that selected had approximate dimensions 0.65 × 0.40 × 0.28 mm. The transmission factors ranged from 0.91 to 1.00. The crystal structure was solved by direct methods using SIR 92 [23] and the structures were expanded using Fourier techniques [24]. The non-hydrogen atoms were refined anisotropically. Some hydrogen atoms were refined isotropically, the remainder were fixed geometrically and not refined. *Crystal data*: $C_{30}H_{27}N_4O_2$, $M = 475.57$, monoclinic, $a = 15.282(8)$, $b = 6.885(1)$, $c = 23.807(4)$ Å, $\beta = 92.44(2)$, $U = 2502(1)$ Å^3, $T = 296.2$ K, space group $P2/n$ (no.13), $Z = 4$, μ(Mo Kα) = 0.81 cm^{-1}, 4591 reflections measured, 4412 unique ($R_{int} = 0.028$) which were used in all calculations. The final R indices were $R_1 = 0.080$, $wR(F^2)$ was 0.232 (all data).

Table 1
Absorption spectral data of **2a** and **2b** in solution

Compound	Solvent	Absorption
		λ_{max}/nm (ε_{max}/dm^3 mol^{-1} cm^{-1})
2a	Benzene	420(31,700)
	1,4-Dioxane	420(25,300)
	Dichloromethane	420(24,200)
	Acetone	420(23,700)
2b	1,4-Dioxane	415(25,100)

Table 2
Calculated absorption spectra for the compounds **2a** and **2b**

Compound	μ/D[a]	Absorption (calc.)		CI component[c]
		λ_{max}/nm	f[b]	
2a	4.97	386	0.89	HOMO → LUMO (86%)
2b	7.08	386	0.89	HOMO → LUMO (86%)

[a] The values of the dipole moment in the ground state.
[b] Oscillator strength.
[c] The transition is shown by an arrow from one orbital to another, followed by its percentage CI (configuration interaction) component.

3. Results and discussion

3.1. Synthesis of naphthooxazole-type fluorophores

Naphthooxazole-type fluorophores **2a** and **2b** are conveniently synthesized as shown in Scheme 1. The 4-aminated-1,2-naphthoquinones **1a** and **1b** in 78 and 56% yield were obtained by refluxing sodium 1,2-naphthoquinone-4-sulphonate with the corresponding 1,4-phenylenediamine in acetic acid in the presence of nickel(II) chloride, respectively. Compounds **1a** and **1b** were then reacted with *p*-cyanobenzaldehyde in the presence of an excess amount of ammonium acetate in acetic acid and gave **2a** and **2b** in 72 and 52% yield, respectively.

3.2. Spectroscopic properties of the naphthooxazole-type fluorophores in solution

The absorption spectra of the naphthooxazole-type fluorophores **2a** and **2b** in solution are summarized in Table 1. The visible absorption spectrum of **2a** was measured in various

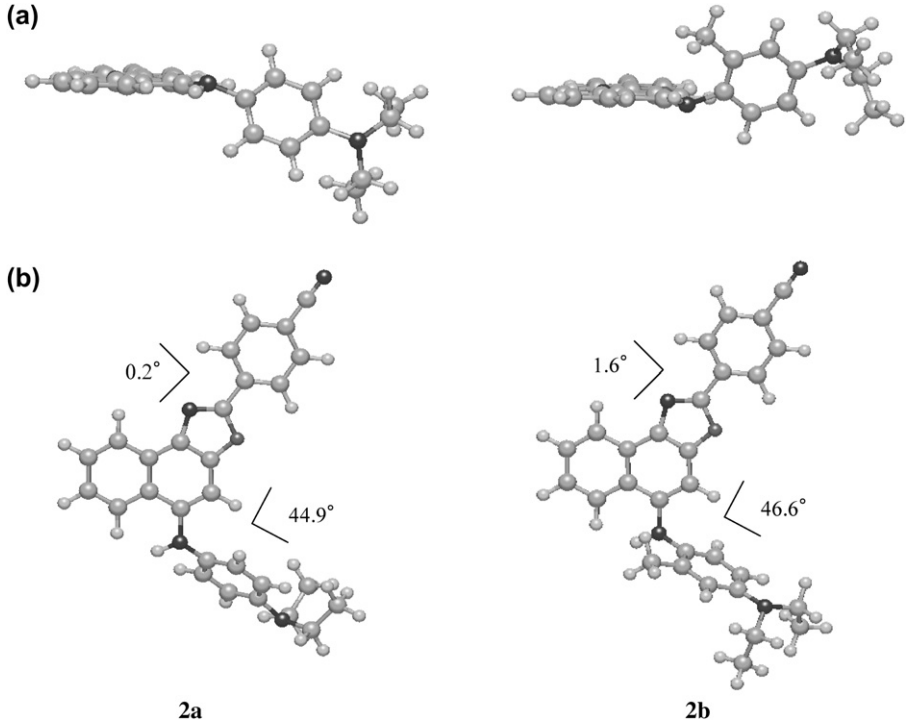

Fig. 1. The optimized geometries of **2a** and **2b** by using MOPAC/PM3 method: (a) a side view and (b) a top view.

solvents, such as benzene, 1,4-dioxane, dichloromethane, and acetone. The fluorophore **2a** exhibited an intense absorption band at around 420 nm (ε_{max}: 23,700–31,700 $dm^3\ mol^{-1}\ cm^{-1}$) in all solvents. Interestingly, the fluorophores **2a** and **2b** did not display fluorescence in solution, but exhibited strong fluorescence in the solid state. Non-radiative decay would be accelerated by free rotation of the 4-diethylaminophenyl ring part of **2** in solution [25,26].

3.3. Semi-empirical MO calculations (PM3, INDO/S)

The photophysical spectra of **2a** and **2b** were analyzed using semi-empirical molecular orbital (MO) calculations. The molecular structures were optimized using the MOPAC/PM3 method [18], and the INDO/S method [19–21] was then used for spectroscopic calculations. The calculated absorption wavelengths and the transition character of the first absorption bands are collected in Table 2. As shown in Fig. 1, the calculated torsion angles between the naphthooxazole ring and the *p*-cyanophenyl group are 0.2° for **2a** and 1.6° for **2b**, respectively, which shows that the two rings are coplanar. Also the *p*-diethylaminophenyl groups are twisted from the plane of the naphthooxazole ring by about 45° for **2a** and 47° for **2b**, respectively.

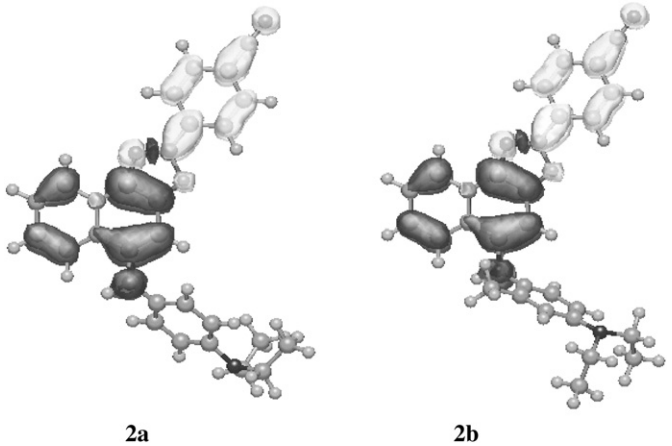

Fig. 2. Calculated electron density changes accompanying the first electronic excitation of **2a** and **2b**. The black and white lobes signify decrease and increase in electron density accompanying the electronic transition. Their areas indicate the magnitude of the electron density change.

The calculated absorption wavelengths and the oscillator strength values are relatively compatible with the observed spectra in 1,4-dioxane, although the calculated absorption spectra are blue-shifted. This deviation of the INDO/S calculations, giving high transition energies compared with the experimental values, has been observed previously [27,28]. The calculations show that the longest excitation bands for **2a** and **2b** are mainly assignable to the transition from the HOMO to the LUMO, where HOMO is mostly localized on the aminonaphtho[1,2-*d*]oxazole moieties and the LUMO on the *p*-cyanophenyl moiety. The changes in the calculated electron density accompanying the first electron excitation are shown in Fig. 2, which show a strong migration of intramolecular charge-transfer character of **2a** and **2b**.

3.4. Inclusion ability in the crystalline state

In order to investigate their inclusion ability, **2a** and **2b** were recrystallized from various organic solvents. The compound **2a** yielded various host–guest inclusion compounds in stoichiometric ratios with guest molecules such as

Table 3
Host–guest molar ratios, crystal form, and colour of the guest-free and guest-inclusion crystals of **2a** and **2b**

Host	Guest	Host:guest (mole ratio)	Crystal form	Crystal colour	Recrysatallization solvent
2a	None	1:0	Needle	Yellow	99% Ethanol
	None	1:0	Needle	Yellow	1-Butanol
	None	1:0	Needle	Yellow	Cyclohexanol
	None	1:0	Prism	Yellow	Ethyl acetate
	DMSO	1:1	Needle	Yellowish orange	DMSO
	Piperidine	3:1	Needle	Orange	Piperidine
	Morpholine	1:1	Needle	Orangish red	Morpholine
	Acetone	2:1	Prism	Red	Acetone
2b	None	1:0	Leaflet	Yellow	99% Ethanol
	None	1:0	Prism	Yellow	Ethyl acetate
	None	1:0	Prism	Yellow	Acetone
	1,4-Dioxane	1:1	Needle	Orange	1,4-Dioxane
	DMSO	1:2	Prism	Orange	DMSO
	Piperidine	1:1	Needle	Orangish red	Piperidine 1
	Morpholine	1:1	Prism	Red	Morpholine

DMSO, piperidine, morpholine, and acetone in the crystalline state; **2b** also gave host–guest inclusion compounds with 1,4-dioxane, DMSO, piperidine and morpholine. The characteristics of the guest-free and various guest-inclusion crystals obtained by recrystallization of **2a** and **2b** are summarized in Table 3. In both cases, **2a** and **2b**, compared to the guest-free crystals, the guest-inclusion crystals varied from yellow to red in colour and a drastic fluorescence quenching was observed (Fig. 3).

3.5. Solid-state fluorescence quenching behaviour upon formation of guest-inclusion crystals

In order to investigate the guest effects on solid-state photophysical properties, the fluorescence excitation and emission spectra of the guest-free and the guest-inclusion crystals of **2a** and **2b** were measured. The spectra recorded at the corresponding excitation and emission maxima of the guest-free and the guest-inclusion crystals are shown in Figs. 4 and 5. The fluorophores **2a** and **2b** exhibited a large red-shift in colour and a drastic fluorescence decrease upon inclusion of guest molecules in the crystalline state. In the case of **2a**, the longest excitation band of the guest-free crystal was observed at 452 nm, however, that of the guest-inclusion crystals was observed at 507–580 nm. In addition, the guest-free crystal exhibited a strong fluorescence band with an emission maximum at 530 nm, whereas the guest-inclusion crystals exhibited weak fluorescence band with an emission maximum

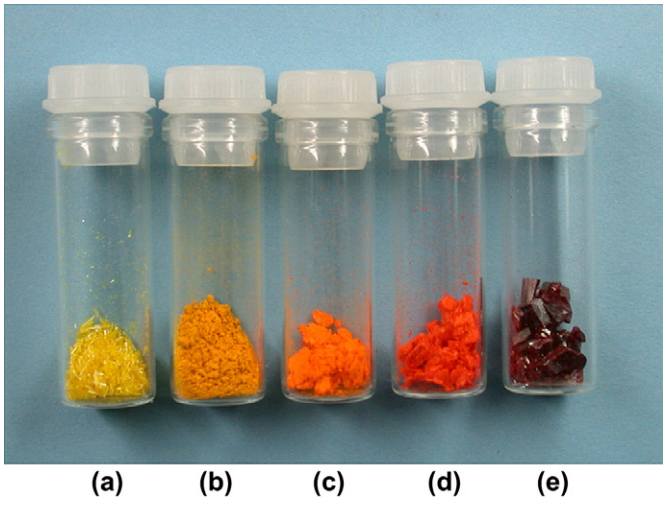

Fig. 3. Crystals of the guest-free and guest-inclusion compounds of the naphthooxazole-type fluorescent host **2a**: (a) **2a** (guest-free), (b) **2a**·DMSO (1:1), (c) **2a**·piperidine (3:1), (d) **2a**·morpholine (1:1), (e) **2a**·acetone (2:1).

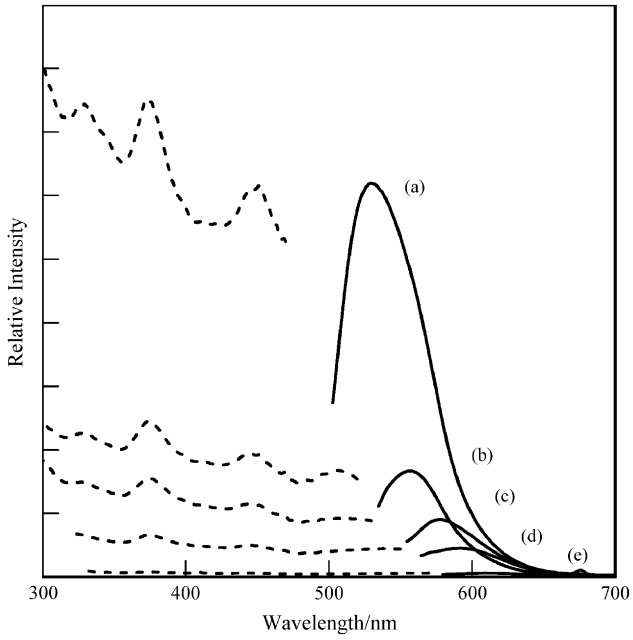

Fig. 4. Excitation (···) and emission (—) spectra of the guest-free and guest-inclusion crystals of **2a**: (a) **2a** (guest-free), $\lambda_{ex} = 452$ nm, $\lambda_{em} = 530$ nm, (b) **2a**·DMSO (1:1), $\lambda_{ex} = 507$ nm, $\lambda_{em} = 558$ nm, (c) **2a**·piperidine (3:1), $\lambda_{ex} = 515$ nm, $\lambda_{em} = 578$ nm, (d) **2a**·morpholine (1:1), $\lambda_{ex} = 538$ nm, $\lambda_{em} = 593$ nm, (e) **2a**·acetone (2:1), $\lambda_{ex} = 580$ nm, $\lambda_{em} = 610$ nm.

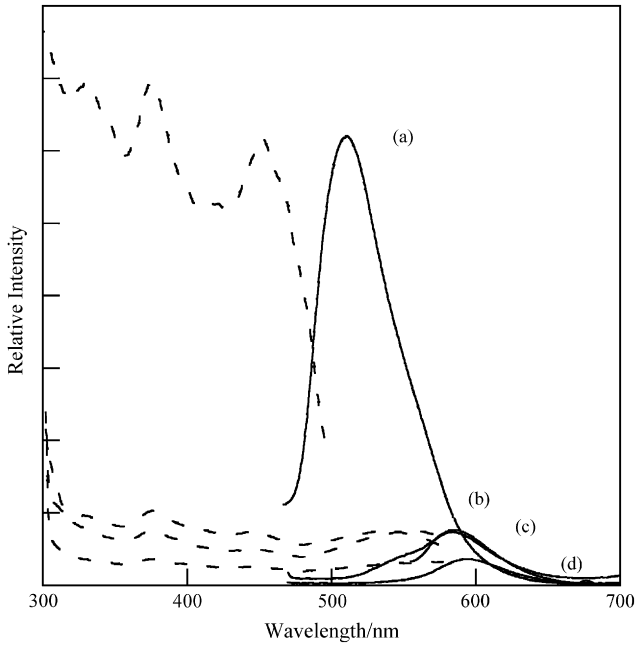

Fig. 5. Excitation (···) and emission (—) spectra of the guest-free and guest-inclusion crystals of **2b**: (a) **2b** (guest-free), $\lambda_{ex} = 452$ nm, $\lambda_{em} = 511$ nm, (b) **2b**·1,4-dioxane (1:1), $\lambda_{ex} = 550$ nm, $\lambda_{em} = 584$ nm, (c) **2b**·DMSO (1:2), $\lambda_{ex} = 552$ nm, $\lambda_{em} = 585$ nm, (d) **2b**·morpholine (1:1), $\lambda_{ex} = 569$ nm, $\lambda_{em} = 592$ nm.

red-shifted to around 558–610 nm. For example, the fluorescence intensity of the guest-free crystal is ca. 100-fold compared to that of acetone-inclusion crystal. In the case of **2b**, similar spectral changes were also observed upon formation of guest-inclusion crystals.

3.6. Relation between the solid-state fluorescence properties and X-ray crystal structures

In order to investigate the enclathrated guest effects on the fluorescence properties of the crystal, the X-ray crystal structures of the guest-free and acetone-inclusion compound of **2a** were studied. The experimental details and crystal data are described in Section 2. The crystal systems were a triclinic space group $P\bar{1}$ with $Z = 2$ for guest-free **2a**, a monoclinic space group $P2/n$ with $Z = 4$ for **2a**·acetone.

The X-ray crystal structures of the guest-free and acetone-inclusion compounds are shown in Figs. 6 and 7. In the guest-free host crystal, face-to-edge and edge-to-edge overlappings are observed between the naphthooxazole and the *p*-cyanophenyl moieties (Figs. 6(b) and (c)). Also, there is a face-to-face overlapping between diethylaminophenyl groups of host molecules (Fig. 6(d)). There are 18 short interatomic contacts of less than 3.6 Å between the host compounds, however, the contacts are almost face-to-edge type of overlap. On the other hand, in the acetone-inclusion crystal as shown in Fig. 7(a), the formation of molecular linking by intermolecular hydrogen bonds between the cyano group of one molecule and the amino group of the next one is observed (NH···N angle = 159.0°, N···N distance = 3.11 Å). In the molecular chain, the host molecules are arranged in the same direction in a given layer and in the opposite direction in the successive layers, which are not observed in the guest-free host crystal. There are two distinct types of face-to-face overlapping, which are covering the whole host molecule through the donor unit of naphthooxazole moiety containing amino group and the acceptor unit of *p*-cyanophenyl group (Fig. 7(b)). The interplanar distances between the naphthooxazole rings are ca. 3.48 Å and

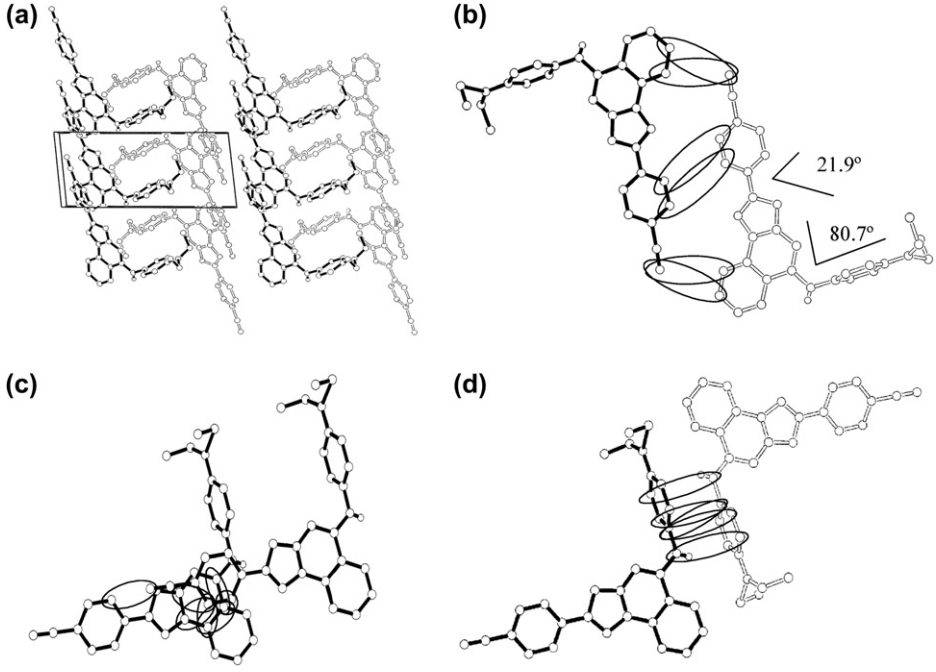

Fig. 6. Crystal packing structure of **2a**: (a) a stereoview of the molecular packing structure, (b) an edge-to-edge overlap, (c) a face-to-edge overlap and (d) a face-to-face overlap between the fluorophores.

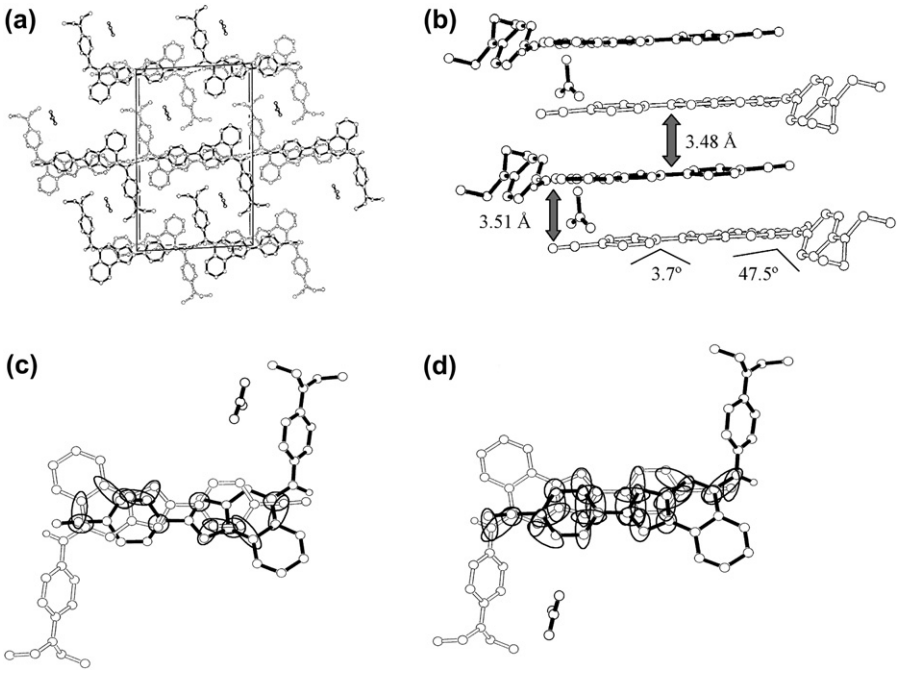

Fig. 7. Crystal packing and hydrogen bonding pattern of **2a**·acetone: (a) a stereoview of the molecular packing structure, (b) a side view and (c) and (d) a top view of a face-to-face overlaps between the fluorophores. The interplanar distance between the naphthooxazole rings is ca. 3.48 Å for (c) and 3.51 Å for (d), respectively.

3.51 Å, and there are 14 and 28 short interatomic contacts of less than 3.6 Å as shown in Figs. 7(c) and (d), respectively, which suggest that much stronger donor–acceptor type π–π interaction exists in the acetone-inclusion crystal than in the guest-free crystal. A large red-shift of the absorption and fluorescence maxima and the solid-state fluorescence quenching by strong donor–acceptor type π–π interactions [12–17,25,26,29–31] and continuous molecular linking by intermolecular hydrogen bonds [16,17] between neighboring fluorophores are known. Consequently, in the acetone-inclusion crystal, it was confirmed that the formation of molecular linking by intermolecular hydrogen bonds and the strong π–π interactions between the fluorophores cause strong fluorescence quenching and a large red-shift of excitation and emission maxima.

Furthermore, from the standpoint of the stereostructure of **2a**, we investigated the effects of the geometric arrangement on the intermolecular interactions. The torsion angle between naphthooxazole ring and *p*-cyanophenyl moiety of **2a** in the guest-free crystal is 21.9°, and *p*-diethylaminophenyl moiety is twisted from the plane of the naphthooxazole ring by 80.7° (Fig. 6(b)). These torsion angles are large compared to those of the optimized geometries by MOPAC/PM3 calculations (0.2° and 44.9° in Fig. 1). On the other hand, as shown in Fig. 7(b), these torsion angles of the molecule in acetone-inclusion crystal are very small compared to those of the molecules in the guest-free crystal. The torsion angles are close to those of the optimized geometries obtained by MOPAC/PM3 calculations. Consequently, the dye **2a** in acetone-inclusion crystal is more planar than in guest-free crystal. It is clear that the small torsion angles of **2a** in acetone-inclusion crystal are attributable to stronger π–π intermolecular interactions than in the guest-free crystal.

4. Conclusions

The novel, naphthooxazole-type fluorophores exhibited a large red-shift and dramatic fluorescence reduction upon inclusion of guest molecules in the crystalline state. Comparison of the X-ray crystal structures of the guest-free and guest-inclusion compounds reveal that the reasons for the red-shift of the absorption and fluorescence wavelength maxima and the drastic fluorescence quenching behaviour upon formation of host–guest inclusion compound of fluorophores **2** are due to strong intermolecular π–π interactions and continuous molecular linking formed by intermolecular hydrogen bonds.

Acknowledgments

This work was partially supported by a Grant-in-Aid for Science and Research from the Ministry of Education, Science, Sport and Culture of Japan (Grant 18350100), by a Science and Technology Incubation Program in Advanced Regions of Japan Science and Technology Agency (JST), and by a Special Research Grant for Green Science from Kochi University.

References

[1] Tang CW, VansSlyke SA. Appl Phys Lett 1987;51:913.
[2] Tang CW, VansSlyke SA, Chen CH. J Appl Phys 1989;65:3610.
[3] Schi J, Tang CW. Appl Phys Lett 1997;70:1665.
[4] Kraft A, Grimsdale AC, Holmes AB. Angew Chem Int Ed 1998;37:402.
[5] Mitschke U, Bäuerle P. Mater Chem 2000;10:1471.
[6] Wong KC, Chien YY, Chen RT, Wang CF, Liu YT, Chiang HH, et al. J Am Chem Soc 2002;124:11576.

[7] Tonzola CJ, Alam MM, Kaminsky WK, Jenekhe SA. J Am Chem Soc 2003;125:13548.
[8] Yeh HC, Chan LH, Wu WC, Chen CT. J Mater Chem 2004;14:1293.
[9] Chen CT. Chem Mater 2004;16:4389.
[10] Chiang CL, Wu MF, Dai DC, Wen WS, Wang JK, Chen CT. Adv Funct Mater 2005;15:231.
[11] Fei Z, Kocher N, Mohrschladt CJ, Ihmels H, Stalke D. Angew Chem Int Ed 2003;42:783.
[12] Yoshida K, Miyazaki H, Miura Y, Ooyama Y, Watanabe S. Chem Lett 1999;837.
[13] Yoshida K, Ooyama Y, Tanikawa S, Watanabe S. Chem Lett 2000;714.
[14] Yoshida K, Ooyama Y, Tanikawa S, Watanabe S. J Chem Soc Perkin Trans 2 2002;708.
[15] Ooyama Y, Nakamura T, Yoshida K. New J Chem 2005;29:447.
[16] Ooyama Y, Yoshida K. New J Chem 2005;29:1204.
[17] Yoshida K, Uwada K, Kumaoka H, Bu L, Watanabe S. Chem Lett 2001;808.
[18] Stewart JJP. J Comput Chem 1989;10:209.
[19] Ridley JE, Zerner MC. Theor Chim Acta 1973;32111.
[20] Ridley JE, Zerner MC. Theor Chim Acta 1976;42:223.
[21] Bacon AD, Zerner MC. Theor Chim Acta 1979;53:21.
[22] teXsan. Crystal structure analysis package. Molecular Structure Corporation; 1985 and 1992.
[23] Altomare A, Burla MC, Camalli M, Cascarano M, Giacovazzo C, Guagliardi A, et al. J Appl Crystallogr 1994;27:435.
[24] DIRDIF94 Beurskens PT, Admiraal G, Beurskens G, Bosman WP, Gelder R, Israel R, Smits JMM. The DIRIF94 program system, Technical Report of the Crystallography Laboratory. The Netherlands: University of Nijmegen; 1994.
[25] Hirano K, Minakata S, Komatsu M. Bull Chem Soc Jpn 2001;74:1567.
[26] Ooyama Y, Yoshikawa S, Watanabe S, Yoshida K. Org Biomol Chem 2006;4:3406.
[27] Adachi M, Murata Y, Nakamura S. J Org Chem 1993;58:5238.
[28] Fabian WMF, Schuppler S, Wolfbesis OS. J Chem Soc Perkin Trans 2 1996;853.
[29] Yeh HC, Wu WC, Wen YS, Dai DC, Wang JK, Chen CT. J Org Chem 2004;69:6455.
[30] Horiguchi E, Matsumoto S, Funabiki K, Matsui M. Bull Chem Soc Jpn 2005;78:1167.
[31] Mizukami S, Houjou H, Sugaya K, Koyama E, Tokuhisa H, Sasaki T, Kanesato M. Chem Mater 2005;17:50.